Preliminary Integrated Analysis of Magnetic Susceptibility, Geochemistry, and Mineralogy in the Neves Corvo VMS District (MAQSIMAL Project)

Introduction

The MAQSIMAL project (Multimodal Airborne Quantum Sensor Instrument for Sustainable Exploration) develops a new generation of quantum sensors for geophysical exploration. The prototype acquires multiple datasets simultaneously, including the 3D magnetic field, magnetic-field gradients and electromagnetic responses (AFMAG/AMT), with high precision over a wide dynamic range (Stolz et al. 2022). Two representative sites were selected for testing (Sweden and Portugal), where prototype data will be compared with existing geological, geophysical and drilling information and targeted ground surveys. The Portuguese site is the Neves-Corvo mining district (Iberian Pyrite Belt, southern Portugal), a world-class but largely concealed VMS system. This extended abstract presents first surface-sample characterisation results from Neves-Corvo, integrating magnetic susceptibility, XRD mineralogy and pXRF geochemistry to evaluate lithological contrasts and alteration footprints relevant to sensor calibration and performance assessment.

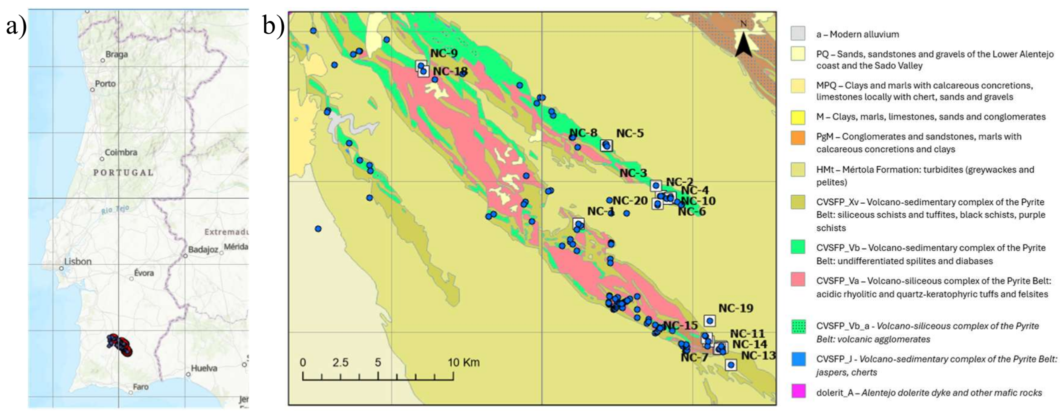

Figure 1 – a) Study area location; b) Geological map indicating measurement sites. Blue dots mark magnetic susceptibility readings. White squeres mark XRD sites.

Geological Setting

Neves-Corvo lies within the Iberian Pyrite Belt (IPB), a major Devonian–Carboniferous VMS province extending from southern Portugal into Spain. Mineralisation is associated with the regional volcano-sedimentary stratigraphy. The Volcano-Sedimentary Complex (VS) is a Paleozoic sequence that hosts the massive sulfide deposits, comprising basic volcanic rocks (altered basalts and andesites, commonly spilites), acidic volcanic rocks (rhyolites, quartz porphyries), chemical sediments (e.g., cherts and jaspers) and interbedded pelites, variably affected by hydrothermal alteration (sericitization, chloritization, silicification, argillitization, etc.). The Flysch Group is a post-mineralization siliciclastic turbidite sequence of late Carboniferous age that unconformably covers the VS Complex, mainly low-grade metamorphic schists and greywackes. The Phyllite–Quartzite Group (PQ) predates the VS and comprises phyllites and quartz greywackes, locally with limestone and dolomite intercalations. The seven deposits occur near the top of the lower VS Complex, with primary Cu–Zn–Pb sulphide lenses at depth (hundreds of metres) (Carvalho et al., 2021; Marques et al., 2022). Surface exposures may preserve indirect expressions of the ore-forming system: oxidation and supergene processes can form Fe-rich gossans (goethite/hematite) that generate Fe-associated geochemical anomalies but typically weak magnetic remanence where magnetite is destroyed. Less altered mafic volcanic rocks may retain magnetite and show higher magnetic susceptibility, providing a basis for relating surface measurements to lithologies and alteration footprints.

Data collection

Fieldwork included magnetic susceptibility measurements with a KT-10 portable kappameter at ~150 outcrops spanning multiple lithologies, alteration styles, and both mineralised and non-mineralised areas (Fig. 1). Multiple readings were acquired per outcrop and summarised as mean susceptibility (K), range (Kmin–Kmax) and standard deviation in SI units. From these sites, 20 samples (NC-1 to NC-20) were collected for XRD mineralogy and pXRF geochemistry.

Magnetic susceptibility

Magnetic susceptibility values show a markedly right-skewed distribution. For the full dataset ($n = 157$), K ranges from 0 to 5.81 $\times 10^{-3}$ SI, with a mean of 0.32 $\times 10^{-3}$ SI and a median of 0.21 $\times 10^{-3}$ SI. Most measurements cluster at low to moderate values (<0.5 $\times 10^{-3}$ SI), while a small number of high values define a long positive tail in the distribution. Magnetic susceptibility varies systematically with lithology (Fig. 2). The highest mean values are associated with basic volcanic rocks (mean ≈ 0.58 $\times 10^{-3}$ SI), which also show the largest dispersion and include the maximum recorded value (5.81 $\times 10^{-3}$ SI). Intermediate volcanic rocks also show relatively high susceptibility, although this group is represented by a single sample. Metasedimentary and sedimentary units are characterized by lower susceptibility values: shales exhibit intermediate K values (mean ≈ 0.27 $\times 10^{-3}$ SI) with wide internal variability, whereas acid volcanic rocks consistently present low susceptibility (mean ≈ 0.12 $\times 10^{-3}$ SI). The lowest values occur in sedimentary and interbedded sedimentary units, with mean K below 0.1 $\times 10^{-3}$ SI.

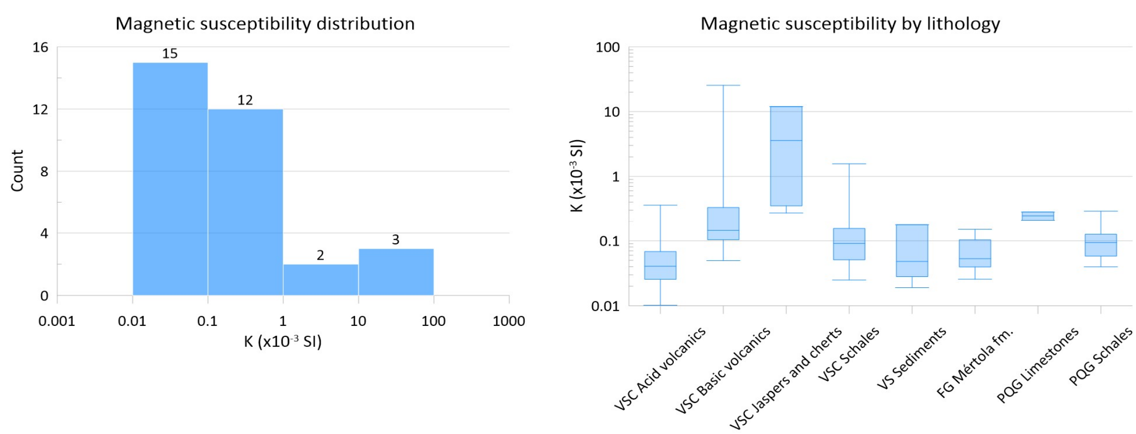

Figure 2 – Magnetic susceptibility distribution for the full dataset (a) and by lithology (b).

XRD analysis

X-ray diffraction data were used to characterise mineral assemblages across lithologies and alteration types. Basic volcanic rocks are dominated by plagioclase and ferromagnesian silicates, often overprinted by alteration phases such as chlorite (e.g. NC-1, NC-3, NC-5, NC-8), alongside albite, augite, and accessory amphibole. Quartz appears as a subordinate phase in some samples (e.g. NC-3, NC-6, NC-9), indicating secondary silica addition. Acidic volcanic rocks, represented by NC-18, are mainly composed of quartz and muscovite/sericite, with no mafic silicates, confirming their felsic nature. Shales and metasedimentary rocks feature quartz–phyllosilicate assemblages, typically quartz and muscovite/sericite (e.g. NC-2, NC-7, NC-11, NC-14, NC-19), with kaolinite and chlorite in some samples, reflecting argillic alteration and low-grade metamorphism. Iron oxides (hematite, goethite) are found in NC-12 and NC-13, indicating oxidising conditions. Cherts and jaspers (NC-4, NC-10) are nearly monomineralic, composed mainly of quartz with minor iron oxides and rare carbonates, consistent with silica-rich sedimentary rocks. The XRD data identify alteration minerals, including muscovite/sericite typical of sericitic alteration (NC-2, NC-6, NC-7, NC-18), chamosite typical of chloritic alteration (NC-1, NC-3, NC-8, NC-17), and kaolinite typical of argillic alteration (NC-7, NC-12, NC-19).

Lithology	Quartz	Feldspars	Primary mafic minerals	Alteration phyllosilicates	Clays	Oxides / carbonates
Jaspers & cherts	Dominant	Absent	Absent	Absent	Absent	Subordinate
Mértola	Dominant	Absent	Absent	Subordinate	Absent	Absent
Basic volcanics	Dominant	Subordinate	Subordinate	Dominant	Subordinate	Dominant
Acid volcanics	Dominant	Absent	Absent	Subordinate	Absent	Absent
Shales	Dominant	Subordinate	Absent	Subordinate	Subordinate	Subordinate

Table 1 – Synthesised mineral assemblages by lithology derived from X-ray diffraction data. Minerals are grouped into major compositional and alteration classes. "Dominant" indicates that at least one sample of the lithology shows the group as a major phase, "Subordinate" indicates presence only as minor or subordinate phases, and "Absent" indicates that the group was not detected.

pXRF measurements

pXRF analyses on the selected samples provide major- and trace-element concentrations used to summarise lithological variability and identify alteration-related geochemical trends (Fig. 3). Across the analysed samples ($n = 20$), major-element distributions differentiate mafic volcanics (Fe–Mg–Ca rich) from schists (Al–K rich) and silica-rich jaspers/cherts (major-element depleted). Trace-element variability includes locally elevated base metals and Sb–Pb, consistent with heterogeneous surface geochemical backgrounds in the district. Relationships among selected elements are summarised using ternary and multivariate representations in Fig. 3. In the integrated subset ($n = 20$), magnetic susceptibility shows a moderate positive correlation with total Fe (Pearson $r \approx 0.49$; $p \approx 0.03$).

Discussion and Interpretation

Integrated measurements show that lithology mainly determines magnetic susceptibility and overall geochemical composition, although hydrothermal alteration can cause localized variations from these typical patterns. Mafic volcanic rocks display the highest and most variable susceptibility, consistent with heterogeneous preservation of magnetite during greenschist-facies alteration. In contrast, felsic volcanic and sedimentary units show uniformly low susceptibility, and samples characterised by sericitic/argillic assemblages are consistently magnetically weak, compatible with magnetite destruction and/or dilution by quartz–phyllosilicate phases. Elemental relationships are also consistent with alteration: K covaries with Al ($r \approx 0.58$) and samples shift towards the Al–K apex of the Si–Al–K ternary diagram, whereas Ca is strongly anticorrelated with Si ($r \approx 0.76$), consistent with spilitisation and/or carbonatisation in mafic protoliths. In the multivariate space, PC1 (36% of variance) separates mafic compositions with positive loadings in Fe, Ti, V, Co, Ni and Ca from felsic/metasedimentary compositions with negative loadings in Si and K, while PC2 (22% of variance) captures enrichment in Al, K, Zn, Ba and Mn ($|\text{loading}| \geq 0.5$) opposed to silica-rich compositions. Covariation among Pb–Zn–As–Sb suggests that a subset of surface samples retains a geochemical signature compatible with VMS-related processes. These conclusions are tentative due to the limited size of the paired subset ($n = 20$) and the semi-quantitative characteristics of pXRF measurements.

Joint consideration of susceptibility, mineralogy and pXRF data increases discrimination between magnetite-bearing mafic lithologies and alteration-dominated rocks. In the present dataset, K tracks Fe at the sample scale ($r \approx 0.49$; $p \approx 0.03$), whereas Al–K enrichment and XRD-identified sericite/kaolinite are associated with low K, supporting the interpretation that magnetically weak responses mark more pervasively altered domains. While limited in scope, the agreement between susceptibility distributions, geochemical trends and XRD assemblages provides an internally consistent basis for initial sensor calibration at the Neves-Corvo test site. Future work should prioritise (i) increasing the number of co-located susceptibility–pXRF–XRD measurements, (ii) improving constraints on sulphide-related vectors (e.g., S where measurable or robust proxy elements), and (iii) evaluating the spatial continuity of these signatures relative to mapped structures and known subsurface mineralisation.

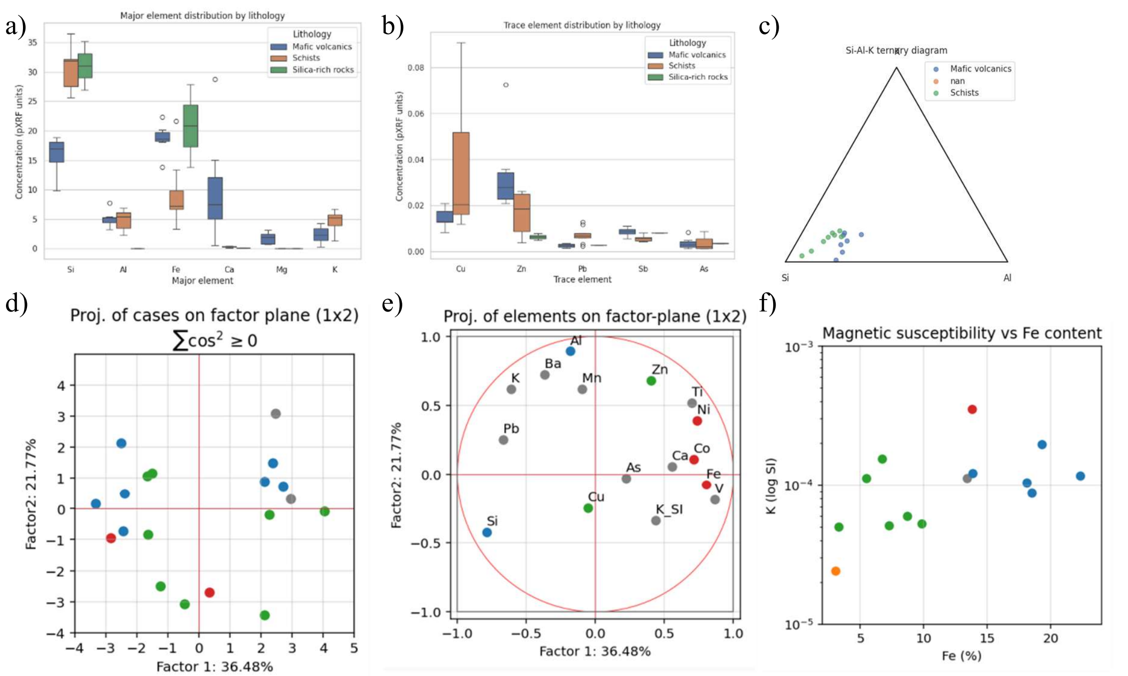

Figure 3. a) Major-element distribution by lithology illustrating compositional contrasts between mafic volcanics, schists, and silica-rich rocks; b) Trace-element concentrations highlighting Pb–Zn–As–Sb variability and Sb–Pb anomalies across lithologies; c) Si–Al–K ternary diagram showing compositional displacement due to alteration; d) PCA of the 20 Neves-Corvo samples (PC1 ≈ 36%; PC2 ≈ 22%); e) Projection of selected elements, including magnetic susceptibility (K_{SI}), on the factor plane (PC1 vs PC2) (|loading| ≥ 0.5); f) Distribution of magnetic susceptibility with Fe content.

Conclusions

Initial MAQSIMAL results at Neves-Corvo show that magnetic susceptibility, XRD mineralogy and pXRF geochemistry provide a coherent basis for distinguishing magnetite-bearing mafic volcanics from magnetically weak felsic/sedimentary rocks and strongly altered domains. The combined signatures are consistent with spatially variable alteration footprints and retain geochemical variability compatible with mineralisation-related processes. These results provide a practical foundation for sensor calibration and motivate expanded paired sampling and spatial mapping to test how well surface variability predicts subsurface VMS-related lithologies and alteration.

Acknowledgements

MAQSIMAL project ERA-MIN3/0001/2023 is acknowledged for financing this study.

References

Carvalho, J., Dias, P., Revaux, C. et al., 2022. A drill-hole, geological and geophysical data-based 3D model for target generation in Neves-Corvo mine region, Portugal. Int J Earth Sci (Geol Rundsch) 111, 403–424 doi:10.1007/s00531-021-02120-x

Marques, F., Dias, P., Carvalho, J. et al., 2022. 3D Constrained Gravity Inversion and TEM, Seismic Reflection and Drill-Hole Analysis for New Target Generation in the Neves–Corvo VMS Mine Region, Iberian Pyrite Belt. Nat Resour Res 31, 2321–2346 (2022). doi:10.1007/s11053-022-10081-4

Stolz, R., Schiffler, M., Becken, M. et al., 2022. SQUIDs for magnetic and electromagnetic methods in mineral exploration. Miner Econ 35, 467–494. doi:10.1007/s13563-022-00333-3